Thermo-mechanical behavior of a thermo-active precast pile

C. de Santiago[1*], F. Pardo de Santayana[1], M. de Groot[1], J. Urchueguía[2], B. Badenes[2], T. Magraner[2], J.L. Arcos[3], Francisco Martín[3]

[1] Laboratorio de Geotecnia (CEDEX) C/ Alfonso XII, 3 y 5. 28014, Madrid (Spain)
[2] Departamento de Física Aplicada. Universitat Politecnica de Valencia. Valencia (Spain)
[3] Grupo Rodio Kronsa. C/ Velazquez, 50-5ª 28001 Madrid (Spain)

A new research and development project has been launched in Spain to undertake some studies on the geothermal use of pile foundations (PITERM PROJECT). The experiment, consists of a specifically designed, constructed and fully monitored geothermal precast pile driven at Polytechnic University of Valencia. The pile is under two types of loads: mechanical and thermal. The mechanical load was applied by means of a mechanical frame anchored to the ground, as element of reaction, and three anchors used to induce an active compressive force. The thermal load was provided by a thermal installation, with a data logger to record the outflow and return temperatures. The testing set is fully instrumented in order to register the thermo-mechanical behaviour of the system in terms of thermally induced movements, thermal axial strain profiles and shaft resistance mobilized as a result of cooling and heating. The results obtained permitted the quantification of three significant effects brought about by the temperature increase: pile uplift, additional load generated in the pile by constrain of the thermal stains, and mobilization of side friction due to the relative displacement of the pile with respect to the ground. The pile strain is of the thermo-elastic type and is strongly affected by the type of surrounding soil.

Keywords: geothermal energy, thermo-active pile, thermo-mechanical behaviour, thermal loads

INTRODUCTION

Energy piles (thermo-active piles or geothermal piles) are foundations with double usefulness: to support the loads of the building and to serve as a heat exchanger with the ground. The geothermal use of pile foundations is a useful, efficient and cost effective method of installing ground heat exchangers for cooling and heating buildings. The key factor in the sustainability of thermo-active foundations systems is utilizing geo-structures that are already needed for structural purposes. This way, coupling piles with ground source heat pumps only requires a low extra over cost for geothermal installation, and it supposes a minimal impact on the piling program. They constitute a growing energy technology that improve the energy efficiency of heating and cooling systems in building and have been widely developed and researched in recent years [1, 2, 3, 4, 5, 6, 7] but it is still necessary to understand how the thermal and mechanical loads affect the mechanical behaviour of the pile. On the other hand, as this is a relatively new technology, robust standards and guidelines have not yet been developed for the design of these systems.

Although it is widely accepted that energy piles foundations are an efficient solution for long-term carbon emission reduction and sustainable construction, they have received only partial acceptance, because of concerns regarding the impact of cyclic thermal changes on their serviceability. In this sense, specific research is still needed to better understand how the thermal loads affect the pile behaviour: changes in vertical strains, stresses and axial loads along the pile, changes in shear stresses between pile shaft and soil, movements at head and toe of pile, changes in soil strength parameters, influence of ground lithological profile and water table position, effects of constrictions at head and toe of pile, possible associated phenomena regarding soil consolidation or negative skin friction, etc.

A research and development project in energy piles was performed in Spain from 2011 to 2015 (PITERM PROJECT). The purpose of this experiment was to improve the knowledge and understanding the effects of cooling and heating on precast piles subjected to mechanical loads in terms of mechanical, geotechnical and thermal actions.

BACKGROUND: PILE-SOIL INTERACTION UNDER MECHANICAL AND THERMAL LOADS

Since the beginning of 1980s, geothermal energy has been increasingly extracted through structural elements in direct contact with the soil [3]. Energy geo-structures have been constructed particularly in Switzerland, Austria, Germany, England and Japan. Two well-documented

* To whom all correspondence should be sent:
cristina.desantiagobuey@gmail.com

thermomechanical tests on full-scale foundations can be pointed out: in Switzerland [1,2], and in the UK [5,6].

The mechanisms of thermo-mechanical effects on energy foundations can be evaluated by assessing data presented by Bourne-Webb et al. [5], who performed a series of thermal and mechanical loading tests on a full-scale foundation at Lambeth College in England, Laloui et al. [2], who performed a series of thermal and mechanical loading tests on a full-scale foundation at the Swiss Federal Institute of Technology in Lausanne, in Switzerland, and Loveridge and Powrie [8], who identified the key factors which influence the heat transfer and thermal–mechanical interactions of such structures and highlighted that the pile aspect ratio is an important parameter controlling the overall thermal performance.

Murphy, K.D. and McCartney [9], focused on the response of two full-scale energy foundations beneath an 8-story building during operation of a heat pump over a 658-day period. During circulation of fluid having temperatures ranging from 7 to 35 °C through the closed-loop heat exchangers within the foundations, the temperature of the reinforced concrete ranged from 9 to 30 °C and was relatively uniform with depth. The thermal axial strains during the first year of heating and cooling were elastic and recoverable, but a change in mobilized coefficient of thermal expansion occurred in the second year, potentially due to changes in interface shear stresses

The coupled thermo-mechanical loads in energy foundation produce unique stress and strain profiles, shown schematically by Bourne-Webb et al. [5]. Under loading alone, the pile is in compression and moves into the supporting soil, and resistance at the pile/soil interface opposes the loading. When a heating cycle is applied, the pile tends to expand, but the surrounding soil will offer restraint to the pile shaft, which will cause compressive axial load developing; at the pile/soil interface, shear induced by heat on the pile/soil interface will oppose that induced by compressive pile loading in the upper part of the pile, but will be additive in the lower. The reverse will happen when the pile is cooled. In both cases the sign of the change in pile/soil interface shear will be opposite in the upper and in the lower part of the pile [5]. Heating a pile subjected to a mechanical load will result in an increase in compression axial load [2, 5] being the pile/soil interface shear stresses modified. Cyclic temperature variations affect in

terms of alteration of the mobilized shaft friction and bearing capacity at the soil-pile interface [10].

All the concepts and information offered by these authors are considered in the analysis of the thermo-mechanical behaviour of the energy pile in this work.

PILE DESIGN AND CONSTRUCTION

A geothermal precast concrete pile was specifically designed and constructed at the Rodio-Kronsa factory (Fig.1).

Fig.1. Precast pile at the factory Rodio-Kronsa

This test pile, made of reinforced concrete with characteristic resistance (f_{ck}) of 50 N/mm^2 and a Young modulus of 31314 N/mm^2 ($E=8500 \cdot (f_{ck})^{1/3}$[11]), with a square cross section of 35 cm side and a total length of 17.4 m, was made of two pieces 8.70 m long each, connected by a joint. To activate it thermally, two polyethylene tubes were installed vertically within a steel pipe, 11.3 cm nominal diameter, located in the centre of the pile with a double U-shaped configuration to allow the passage of the heat carrier fluid.

Ground conditions of the testing site in Valencia and mechanical ground properties (Table 1) were taken into account for the foundation design: A superficial fill layer of sandy gravel (1m thick); a second layer of stiff clay (1 m thick); a 6 m thick layer of soft and black organic clays; and below depth 8 m, layers of sandy gravels extended up to a depth of at least 27 m, interlayered with some stiff clays levels. The ground water table is located at a depth of 2.0 m. Under these lithological conditions, the pile should work transferring loads to the soil levels located at more than 11 m of depth.

Table1. Material parameters

Depth (m)	Lithology	Geotechnical Parameters
0 – 1.00	Sandy gravel	ρ_{ap} = 18 kNt/m³ c' = 0 kPa φ = 28º
1.00 – 2.00 F.L ∇	Stiff clay	ρ_{ap} = 20 kN/m³ c' = 1 kPa φ = 26º c_u = 30 kPa
2.00 – 7.80	Soft and black organic clays	ρ_{ap} = 19 kN/m³ c' = 5 kPa φ = 26º c_u = 20 kPa
7.80 – 26.0	Sandy gravels	ρ_{ap} = 22 kN/m³ c'= 0-20 kPa φ = 35º c_u = 30 - 50 kPa

The ultimate compressive resistance of the pile, calculated from ground test results by the method established in the Spanish Building Code [12], was 2568 kN. Subsequently, a service compression load of 1000 kN was decided at the pile head.

The pile was fully instrumented before being cast in the factory. The aim of the instrumentation was to monitor the distributions of temperature and axial strain with depth, as well as the supply and return temperatures of the heat exchanger fluid. Pairs of vibrating wire concrete-embedment strain gauges (VWSG) (GS2100 Geosense) with a gauge factor of 3.51 and a coefficient of linear thermal expansion of the steel wire in the gauges of 12.2 $\mu\varepsilon$/°C ,were oriented longitudinally and attached to the lateral reinforcing bars at seven different depths along the pile, then cast in concrete during construction (Fig.2). Each VWSG contained a thermistor to monitor temperature in the concrete at each sensor location.

Fig.2. VWSG attached to the reinforcement bar

With the aim of comparing with the conventional instrumentation, Optical Fibre Sensors (OFS) (Micron Optics, OS3600), based on fiber Bragg grating (FBG) technology providing integrated temperature compensation, were installed to measure temperature and vertical strain

each 2 m along the length of the pile. Schematics of the foundation, the embedded sensors and the geological profile are shown in Fig.3 and Fig.4.
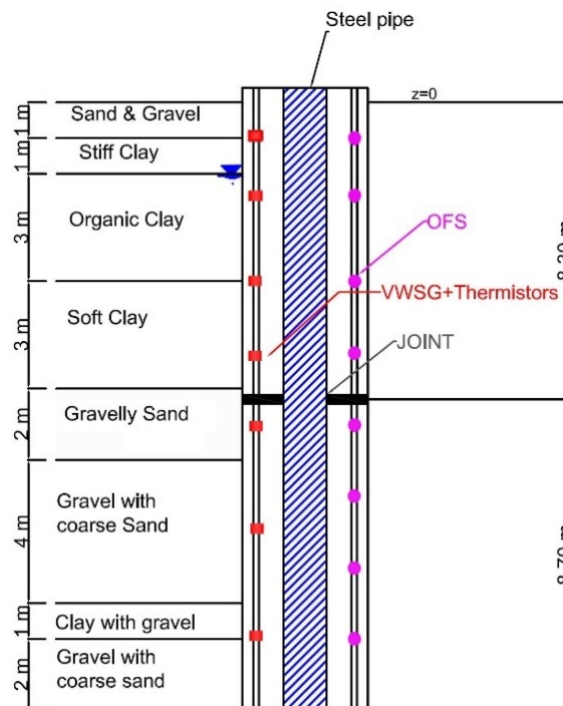
Fig.3. Soil profile and instrumentation
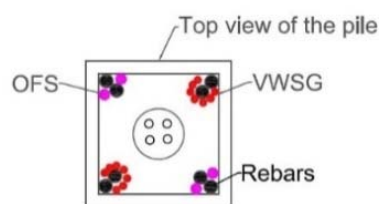
Fig.4. Top view of the pile

EXPERIMENTAL SET UP

The pile was driven in the ground the 27th of June, 2012 in Valencia. Using CAPWAP® (Case Pile Wave Analysis Program) software the total bearing capacity of the pile, as well as the resistance distribution along the shaft and at the toe were calculated during the driving, by means of the Pile Driving Analyzer (PDA) system . The program takes as input the force and velocity data obtained with dynamic load tests. These tests were carried out to assess the ultimate vertical compressive resistance, resulting in a base resistance of 1800 kN and a shaft resistance of 711 kN.

The pile was then subjected first to two static load tests (test A and test B), and secondly to thermal tests by maintaining the mechanical service load of 1000 kN(test C). Therefore, two types of load application systems were needed: mechanical and thermal.

43

The mechanical load was applied by means of a metallic frame, as element of reaction, fixed to the ground by means of three 25 m long anchors, with an inclination of 5º. The compressive force was applied to the pile head by a hydraulic jack. A calibrated load cell measured the real load throughout the test (Fig.5).
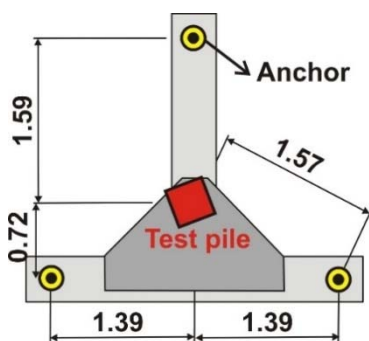
Fig.5. Scheme of the mechanical loading system

The thermal load was provided by a thermal installation (Fig.6), including a reversible air-source heat pump, a tank, a three-way valve for temperature regulation of the water entering into the EP, a flowmeter and a number of temperature probes with a data logger system to record the inflow and outflow temperatures during the test.

Once the pile was driven into the soil and thermally activated, the steel pipe located in the centre of the pile was filled with high thermal conductivity mortar (λ = 2.1 W/mK) made up of quartz sand and sulphate resistant cement. The characteristic resistance of this grout material is almost equal to that of the concrete used in the pile.

The initial temperatures recorded by all the sensors prior to start the initial load test were between 17ºC and 21ºC. Below 10.40 m depth the ground temperature remains constant at 19ºC.

Finally, additional displacement sensors were located outside the pile, in strategic points of the loading frame and anchors, in order to monitor the pile behaviour during the thermal and mechanical loads (Fig.6 and Table 2).

The Fiber Optics Sensors, based on fiber Bragg grating (FBG) technology, are intended exclusively for embedding in concrete structures. Although the technical sheet of these sensors offer nominal wavelength for 22ºC (λ_{22}) and a temperature sensitivity constant value (S_t) of 23.8 pm/ºC, a lab-calibration was performed prior to their installation within the energy pile. In this manner, all the individual real λ_{22} and S_t values were determined to allow the later conversion of the raw signals into temperature and strain values.
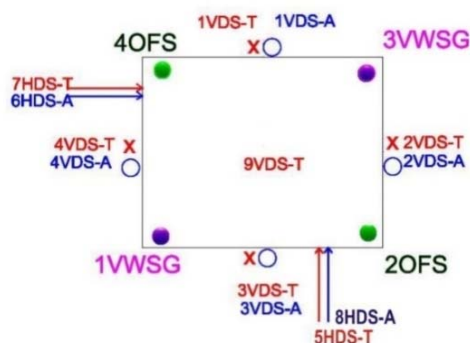
VDS-$_T$: Vertical displacement transducer: LVDT
VDS-$_A$: Vertical displacement analog dial gauge
HDS-$_T$: Horizontal displacement transducer: LVDT
HDS-$_A$: Horizontal displacement analog dial gauge
OFS: Optical fibre sensors
VWSG: Vibrating wire strain gages

Fig.6. External sensors on the pile head

Table 2. Total monitoring during the study

Test element	Monitoring
Test pile (external)	4 analog dial gauges for vertical pile head displacements 4 electronic transducers (LVDT) for vertical pile head displacements 2 analog dial gauges for horizontal pile head displacements 2 electronic transducers (LVDT) for horizontal pile head displacements 1 LVDT to loading frame Load cell
Test pile (internal)	VWSG at seven levels in rebars diametrically opposed over 17 m length of pile OFS cables, 2 loops for strain and temperature measurement at the same time placed each loop diametrically opposed
Anchors	VWSG in each anchor to measure strain and temperature

As for the VWSG sensors, the ideal methodology to measure the global thermal correction factor would have involved measuring the axial heave of the energy pile during heating before applying the mechanical load of 1000 kN and comparing this with the measured thermal axial strains using a soil-structure interaction analysis such as that of Knellwolf et al. [13]. In the absence of this type of test, the calibration factor given by the factory (11 µɛ/ ºC) was used in calculations.

FIELD ASESSMENT OF THERMAL PERFORMANCE

Energy pile (EP) design needs to integrate geotechnical, structural and thermal considerations. The geothermal heat exchange capacity of an

energy pile is a key design parameter to dimension the geothermal loops and the heat pump system. Thermal characteristics of the ground as well as the heating and cooling loads from the structure need to be considered for the number of EPs that will be utilized as heat exchangers. Therefore, the thermal properties of the site need to be evaluated in addition to the geotechnical characterization for foundation design. In this project, the first test performed to evaluate the thermal behaviour of the experimental EP has been a thermal response test (TRT).

TRT is a widely used field method for estimating soil thermal conductivity and the thermal resistance of traditional borehole heat exchangers (BHE). However, there is a lack of scientifically supported guidelines for analysing TRT data from energy piles [14]. Recently, the Ground Source Heat Pump Association (GSHPA) published a manual on the design and construction of energy piles [15], including TRT guidelines for EP. Testing methods for BHE systems assume a high length to diameter ratio so that the shape of the borehole approaches a line source. The diameter of an energy pile is significantly larger and the depth is typically much less. The difference in geometry means that the testing practices of BHEs do not necessarily apply to EPs, for this reason, the GSHPA association has made some recommendations in regards to conducting TRTs for EP systems:

1. When the potential use of EP systems is identified early in the design process a BHE can be constructed with a single loop and tested to find the local thermal properties.

2. If the designed piles are no larger than 30cm in diameter, a TRT can be carried out using the recommendations made for a BHE system.

3. If the EP system design consists of piles larger than 30 cm in diameter, the TRT should be extended to ensure that the thermal resistance of the pile is overcome. Furthermore, more sophisticated interpretation techniques can be applied.

4. Once the EP is fully instrumented with strain gauges and temperature gauges, it is possible to conduct a complete stress-strain analysis as well as a thermal analysis in order to better understand the structural and thermal behaviour of the pile under the superimposed action of coupled mechanical and thermal loads.

Since the experimental energy pile has a 0.35 m side square section, and bearing in mind the recommendations of GSHPA, the field assessment of thermal performance in this project consists of

two different tests: firstly, two bespoke TRT of longer duration (5 + 6 days) were performed to ensure that the thermal resistance of the pile is overcome. Then, as the EP is fully instrumented with VWSG extensometers, thermistors and Fiber Optics Sensors, a complete stress-strain analysis was undertaken in order to better understand the structural and thermal behaviour of the pile under the superimposed action of coupled mechanical and thermal loads.

Thermal loads generating facility

The main objective of the facility is to produce the thermal heat injection and to monitor the associated variables that allow to perform the thermal response test analysis.

In order to produce thermal loads, the appliance uses a reversible heat pump (cooling) or a thermal resistance (heating) and a hydraulic circuit. Several measurement elements and electronic circuits are necessary for the required data-logging and measurement control. The facility is shown in figure 8 schematically.
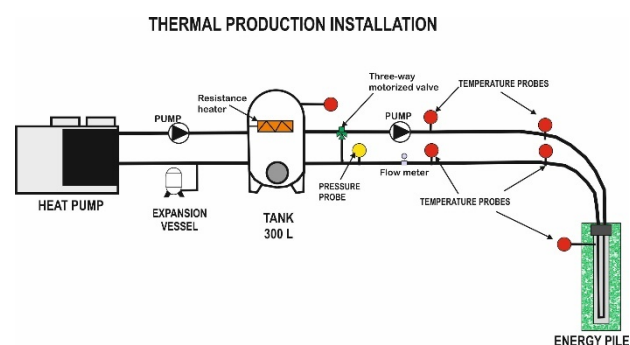
Fig.7. A scheme of the thermal loading system

The air-water-heat pump (AWHP) allows to heat or cool down the water entering into the pile, whereby the control system fixes the temperature difference between entering and outflow water temperature, thus allowing to keep a constant heat flux within the EP.

Throughout the test, water is circulated into the EP and heat is exchanged with the surrounding soil through the pipes located inside, in a thermo-hydraulic configuration alike any conventional BHE. For that purpose, the system comprises two water loops:

• The primary loop, which contains the heat exchanger pipes, installed in the pile, the primary circulation pump, a three-way valve for regulating the temperature of the injected water, a flow meter and various temperatures probes;

• The secondary loop, comprising the heat pump, a storage tank equipped with a thermal

resistance, an expansion vessel and the secondary circulation pump.

The primary loop is responsible for maintaining a constant heat flux to the EP, by keeping a constant temperature difference between inlet and outlet flow. The secondary circuit supplies heated or chilled water either by the thermal resistance or the AWHP.

The temperatures of the heat exchange fluid entering and exiting the pile during heat pump operation were monitored using pipe-plug thermocouples installed in the inlet and outlet ports of the manifold. The facility is able to extract or inject heat at constant rates into the ground depending on the relationship between the temperatures of the heat carrier fluid and the ground around the pile. Summarizing the main characteristics of the facility:

- Cold generation (heat pump) and heat generation (electric resistance).
- Regulation of the injected power by means of pulse width modulation.
- Monitoring of the flow, inlet and outlet temperature and pressure.
- Remote control of the process.
- Data logging.

Thermal characterization of the pile

The thermal characterization of the experimental pile was done by a heat injection test, simulating the thermal pile behaviour working in cooling mode. Once the working load was applied (1000 kN), two heat injection tests were performed to characterize the installation. Taking into account the EP geometry (Table 3) and the GSHPA recommendations [11], the tests duration was longer than usual. The extended testing time ensures that the pile thermal resistance has reached a near steady state behaviour.

Table 3. Geometry of the tested energy pile

Pile length (m)	17.4
Square cross section side (m)	0.35
Active pipe length (m)	17
Heat exchanger type	Double U
Number of pipes	4
PE Pipe Outer Diameter (m)	25.0
PE Pipe Inner Diameter (m)	20.6

The EP characterization was carried out during 11 (5+6) days by introducing different heat injection levels to the experimental pile (700 and 1400W). The temperatures of the heat exchange fluid entering and exiting the EP during heat pump operation were monitored using pipe-plug

thermocouples installed in the inlet and outlet ports of the manifold. In this way, checking the temperature variations of the inlet and outlet pipes allowed to obtain the evolution of temperature over time. The main test parameters are shown in Table 4.

Table 4. Thermal response test parameters

	Test 1	Test 2
Inflow-outflow temperature increase	1ºC	2ºC
Flow rate	0.6 m³/h (10 l/min).	0.6 m³/h (10 l/min).
Heat carrier fluid	Tap water	Tap water
Nominal heat injection rate	700 W	1.400 W
Nominal specific heat injection rate	40 W/m	80 W/m
Test duration	5 days	6 days

For the thermal analysis as conventionally used to analyse TRT tests, the EP is approximated by a line source in an homogeneous semi-infinite medium. In this so called *infinite line source approximation (ILS)*, the evolution of the mean fluid temperature $T_f(t)$ would follow the trend described by the following equation (1) [16]:

$$T_f(t) - T_0 = \frac{q_c}{4\pi\lambda}\left(\ln\left(\frac{4\alpha t}{r_b^2}\right) - \gamma\right) + q_c \cdot R_b =$$
$$= \frac{q_c}{4\pi\lambda}\ln(t) + q_c\left[R_b + \frac{1}{4\pi\lambda}\left(\ln\left(\frac{4\alpha}{r_b^2}\right) - \gamma\right)\right] \quad (1)$$

Where q_c represents the constant heat injection rate used for the response test (W/m), T_0 the undisturbed ground temperature (ºC), t denotes time after start of the heat injection (s), r_b the borehole (pile) radius and γ is Euler's constant (0.5772). The so-called borehole resistance, R_b, is an important design parameter and represents the short-term thermal response of the system.

A maximum error of a 10% for $t \geq 5r^2/\alpha$ is generally accepted in thermal response test applications [17].

For a proper analysis, the previous equation is adapted to the equation for the line (2):

$$T_f(t) = k \cdot x(t) + m \quad (2)$$

- where k is the slope of the line and it is related with the ground thermal conductivity according to the following expression:

$$k = \frac{1}{4\pi\lambda} \quad (3)$$

- and m is the coordinate in the origin, which represents the value when the time is equal to 0.

Considering the thermal resistance of the borehole a constant value over time:

$$m = T_0 + R_b q_c \qquad (4)$$

- and finally, the time-dependent term:

$$x(t) = q_c \left(\ln\left(\frac{t}{t_0}\right) - \gamma \right) \qquad (5)$$

Being $t_0 = \frac{r_0^2}{4\alpha}$

It is clearly evident that the equation (1) corresponds to equation (2) using the values in (3), (4) and (5).

The measurements recorded during the tests allow to infer the ground thermal conductivity and the pile thermal resistance by means of a heat transfer model such as has been described above. Fig.8 shows the evolution of the average fluid temperature against time recorded during testing.
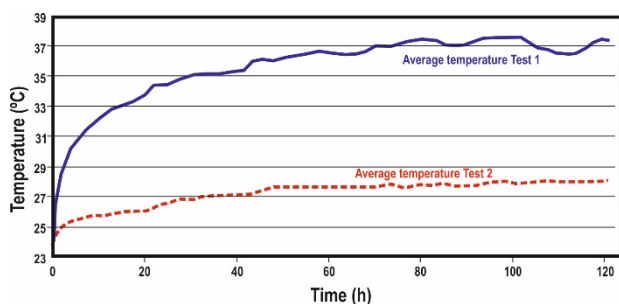
Fig.8. Average fluid temperature throughout TRT

As the evolution of the fluid temperature is logarithmic (Fig. 9), the ground thermal conductivity (λ) can be evaluated by plotting the fluid temperature against ln (t) and determining the slope of the line k:

$$\lambda = \frac{q_c}{4\pi k} \qquad (6)$$

$$x = Q_2 \left(\ln\left(\frac{t}{t_0}\right) - \gamma \right)$$
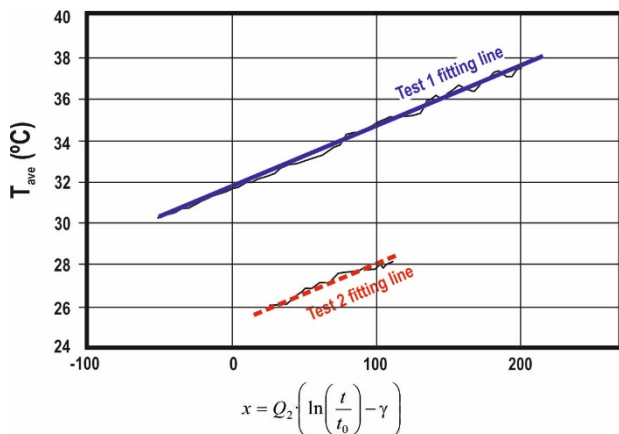
Fig.9. Semi logarithmic graph of average fluid temperature versus ln (t)

The equations obtained for the two test performed were:

$$\text{Test 1: } 0.029x + 31{,}7$$

$$\text{Test 2: } 0.029x + 25{,}3$$

The slope of the line is the same in both tests, as it only depends on the ground thermal conductivity:

$$k = \frac{1}{4\pi\lambda} = 0.029$$

resulting in:

$$\lambda = 2.7 \pm 11.7\% \text{ W/mK}$$

Once the ground thermal conductivity is known, the pile thermal resistance can be assessed on the basis of equation 3. This requires knowledge of the undisturbed ground temperature. In this case, assuming that T_0 is the same in both tests, the energy pile thermal resistance (R_b) can be determined independently of the undisturbed ground temperature giving rise to:

$$R_b = 0.16 \pm 11.7\% \ mK/\text{W}$$

Compared to other works [18, 19, 20] the EP thermal resistance value calculated is in line with existing data, as shown in the following table (Table 5).

Table 5. Energy pile thermal resistance values

EP characteristics	Rb (mK/W)
Concrete driven Square cross section 0.27x0.27 m² Simple U pipe	0.17
Continuous auger pile 0.3 m Simple U pipe	0.22
Precast high strength concrete 0.4 outer and 0.12 inner hollow W shape pipe	0.131
Precast high strength concrete 0.4 outer and 0.12 inner hollow 3U shape pipe	0.098

THERMO-MECHANICAL BEHAVIOUR OF THE PILE

Geotechnical design requires consideration of the complex interaction between temperature change and induced stresses and strains in the foundation, which may affect building performance. Specifically, contraction or expansion of the foundation during cooling or heating may lead to mechanical distress movements of the structural foundation elements or the building itself, as well as changes in pile shaft shear stresses and

base loads and, therefore, in the factors of safety for bearing resistance of the foundation. An important aspect of this study was to evaluate thermally induced axial strains and stresses in the energy foundations caused by temperature changes.

The parameters measured and registered by VWSG and FOS were quite similar, both in relative values and in trends with depth and temperature.

The first step to define the thermal axial strain is to isolate the effect of the mechanical loading. To achieve this, an initial measurement was performed under a mechanical load of 1000 kN, without any temperature action upon the pile. From this initial measurement onwards, the value of mechanical component of the strain after this point is considered constant, assuming that there is negligible variation in the mechanical load applied to the pile head over time. Accordingly, the measured strain values ε_m were zeroed by subtracting the mechanical axial strain. Next, the zeroed strain values were corrected for the differential thermal deformation between the gauge (steel) and the concrete, in which it is embedded, by means of: $(\alpha_{gauge} - \alpha_{concrete})\Delta T$, where α_{gauge} is the coefficient of linear thermal expansion of the steel wire in the gauges (-12.2 $\mu\varepsilon$/°C); $\alpha_{concrete}$ is the coefficient of linear thermal expansion of the concrete(11$\mu\varepsilon$/°C) and ΔT is the temperature change of the pile.

"Test C" is meant to show the thermo-mechanical behaviour of the pile under a constant and stable mechanical load of 1000 kN and a wide range of thermal loads, simulating its use within a geothermal installation working on summer mode (cooling the building and heating up the foundation). This test was performed between 26th of June and 10th of July of 2013, following the procedure and stages shown in Fig. 11. These three stages correspond to different heat injection rates by applying different heating rate values (Table 6).

Table 6. Stages of the test C

	Stages		
	1	**2**	**3**
Initial date	26/6/2013	01/7/2013	05/7/2013
Initial hour	11:09	12:33	12:03
Final date	01/7/2013	05/7/2013	10/7/2013
Final hour	11:06	11:12	13:30
Fluid	Tap water		
ΔT°C	1°C	3°C	1.5°C
Heating power (W)	700	2100	1050
Heat injection rate (W/m)	40	120	60

In order to define profiles of thermal axial strain representative of the pile performance, some specific moments in time were identified. All of them were chosen at the end of each thermal stage, after a time enough to reach thermal equilibrium in the system (Table 7 and Fig.10).

Table 7. Strategic moments identified during test C

Moment	*Date and hour*	*Observations*	*Surface temperature(°C)*
Static load test B	29/05/2013	To compare and validate both types of sensors before test C. After test B the pile head load was kept constant at 1000 kN until completion of all the experimental study.	
C0	26/06/2013 10:57	Prior to test C	22.9
Ca	01/07/2013 12:27	After thermal equilibrium at stage 1	30.4
Cb	05/07/2013 12:27	After thermal equilibrium at stage 2	32.3
Cc	10/07/2013 14:30	After thermal equilibrium at stage 3	26.2
Cd	11/07/2013 11:54	End of test C	23.1
Ce	30/07/2013 10:07	19 days after end of test C	29.8
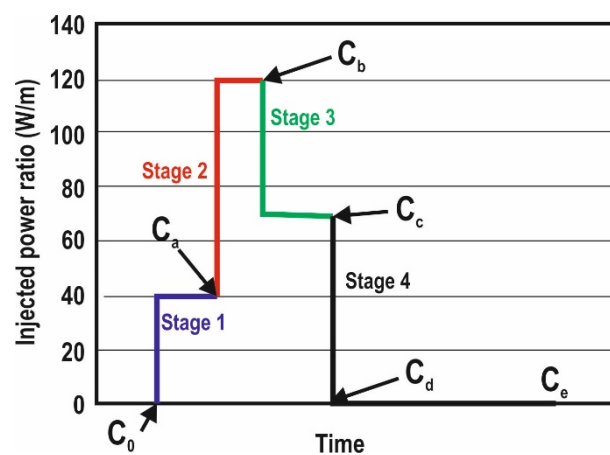
Fig.10. Schematic of the test C and identification of strategic moments: C_0, C_a, C_b, C_c, C_d and C_e.

Throughout test C, strains and temperatures, power and flow were registered, to be able to analyse any possible out of phase results regarding the thermal and the geotechnical behaviour of the pile.

Temperatures

Firstly, all the profiles obtained during the test show a temperature decreasing with depth (Fig.11).

Near the surface the pile temperature is affected by both the injected thermal power and the atmospheric temperature variations. This phenomenon, well explained by McCartney & Murphy [21] and Bourne-Webb [5], is less significant when larger depths are considered, less affected by atmospheric temperature changes.
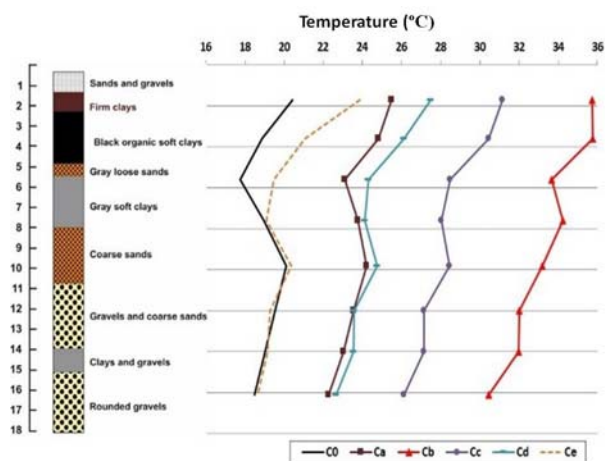
Fig.11. Temperature profile evolution during test C

Prior to starting the test C (C0), the ground temperature is more or less homogeneous around 19-20ºC. Once the test begins, the effect of heat injection in the temperature profile of the pile is clear: in Cb (after 120 W/m heat injection rate equilibrium is achieved) the temperature is 35-36ºC in the upper meters and 30-31ºC in the lower zone. In terms of temperature changes, comparing these values to the moment C0, the first meters of pile show a temperature increment of 17ºC, while 12ºC change is registered in the lower part of the pile. In Ca (after 40 W/m heat injection rate thermal equilibrium is achieved) the temperature profile is close to the one corresponding to Cd, after finishing the test. This highlights the fact that the pile needs some time to dissipate the heat generated during heat injection. In Ce, after 19 days of thermal stabilization, the temperature profile comes back to the initial state (C0) in the deeper part of the pile. The 6 most superficial meters the Ce profile shows higher temperature values than the C0 profile. This is due to the different climatological conditions and ambient temperatures. While in C0 (26th of June) the ambient temperature was 22.9ºC, in Ce (30th of July) it was 29.8ºC.

Fig.12 shows the thermal evolution of the pile in terms of temperature change with respect to C0. The close shape of the response at different depths along the pile shows a strong dependence of the thermal temperature changes on the heat injection rate at the different stages of the test.
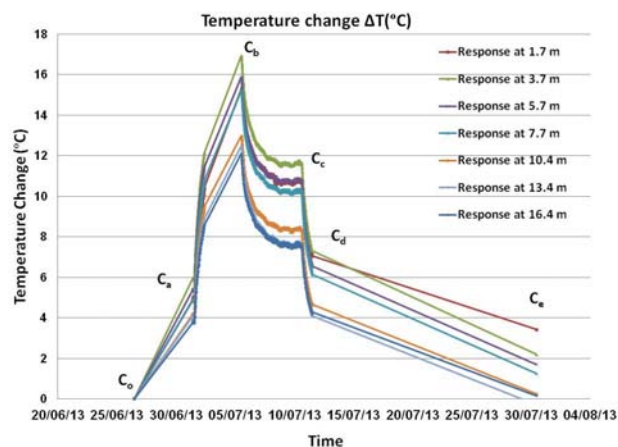
Fig.12. Temperature change detected at different depths throughout the test stages

Pile head movements

The sensors installed at the pile head allowed to measure in real time the vertical and horizontal movements generated due to thermal changes during the test C (Fig.13 and Fig.14).
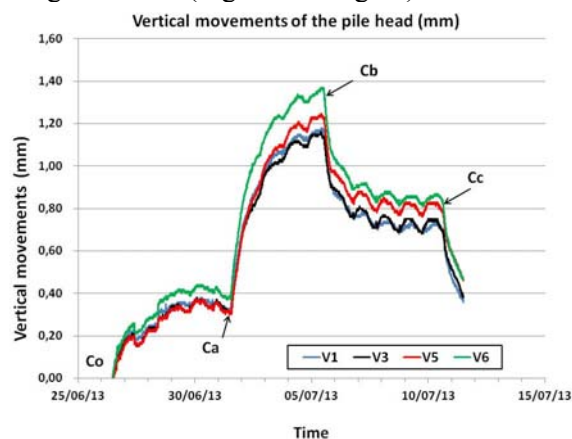
Fig.13. Vertical movements of the pile head during test C

The maximum vertical movements measured at the pile head were 0.4 mm in Ca (40 W/m injected), 1.4 mm in Cb (120 W/m injected), and 0.8 mm in Cc (70 W/m injected). After this moment, all the sensors showed a trend to diminish towards zero as the pile thermally recovered. Furthermore, a clear cyclic oscillation due to thermal daily variations can be detected. The pile head did not return to its original elevation upon cooling (Cd), but maintained an upward displacement of approximately 0.4 mm.

The horizontal movements of the pile head (Fig. 14) do not show the same clear correlation to the sequence of different stages throughout test C as vertical movements do.

Fig.14. Horizontal movements of the pile head during test C

Fig.15. Theoretical thermal unrestrained strains in a completely free of movements pile ($\varepsilon_{th,f}$)

TH2 sensor measured a movement towards a maximum value of +0.6 mm, while TH4 sensor moved towards -0.3 mm. These two components give a resulting movement of 0.65 mm towards South-Southeast. Daily oscillation are quite evident.

Strains

When a pile under working load is heated or cooled, a complex behaviour is imposed upon the pile that varies with ground conditions and different degrees of end restraints. Heating induces expansion while cooling induces contraction leading to pile vertical strains, displacements of the pile head and changes in shaft friction and base stresses. The total strain due to mechanical and thermal loads (ε_T) is:

$$\varepsilon_T = \varepsilon_m + \varepsilon_{th} \qquad (7)$$

where ε_m is the strain due to a mechanical load and ε_{th} is the strain due to the thermal loads.

1. Thermal free strains

Thermal deformations (Fig.15) may occur in energy foundations due to thermo-elastic expansion, in which thermal strain ε_{th} occurs during a change in temperature proportionally to this change, by means of a coefficient of thermal expansion. Considering a theoretical unrestrained pile, the change in temperature induces a uniform free strain [22]:

$$\varepsilon_{th,f} = \alpha_{pile} \cdot \Delta T \qquad (8)$$

α is the coefficient of thermal expansion of the pile (11 µε/°C) and ΔT the variation of temperature between the initial moment (CO) and the different stages during test C (Fig.13).

2. Observed strains

Actually, the energy pile is far from unrestrained. The surrounding soil provides a confining effect on the pile, constraining the possible deformations. For this reason, depending on soil-structure interaction conditions, the real expansion or contraction observed and measured (ε_{obs}) by the VWSG extensometers within the energy pile due to the applied thermal loads results much lower than the theoretical free thermal unrestrained strains calculated previously from the temperature change measured in the pile.

$$\varepsilon_{obs} = \varepsilon_{final} - \varepsilon_{initial} + \alpha_{gauge} \cdot \Delta T \qquad (9)$$

where α is the coefficient of thermal expansion of the gauge (12.2 µε/°C) and ΔT the variation of temperature between the initial moment (CO) and the different stages during test C (Fig.13).

The profiles of observed axial strain induced by the thermal loads corresponding to the specific moments defined above are shown in Fig. 16. In these figures, negative strains indicate compression in the pile, while positive strains indicate expansion.
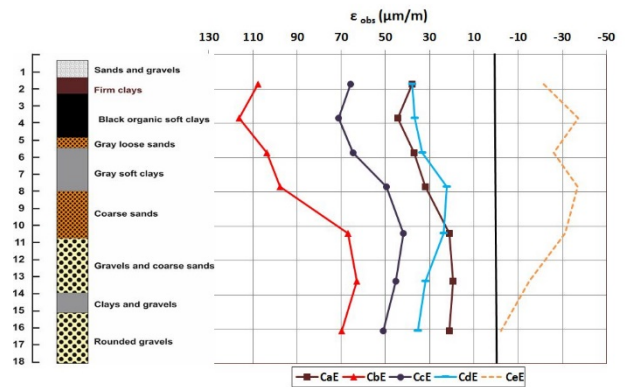
Fig.16. Observed deformation, measured by the VWSG extensometers

Regardless of the shapes of the mechanical strain profiles, it is clear that the heating operation led to a shift in the observed strain profiles to the left, towards positive values (expansion). Cooling after the test leads to a recovering and shift of the profile to the right, towards negative values (compression).

All the curves show positive values, corresponding to tensile strains, with the exception of the Ce profile, corresponding to 19 days after finishing the test C, where a 38 μm/m maximum compression strain was registered. The maximum tensile deformation is measured in Cb, when the heat injection is maximum, as well as the temperature measured in the pile. In Cd, just after the interruption of heat release, a 40 μm/m tensile strain was measured. The shape of the strain profiles depends not only on the temperature changes, but also on the resistance the ground around the pile offers to its deformation. With this view, larger deformation values are measured in the upper part of the pile, at all the heat injection curves, while the deeper part of the pile tends to show lower strain values. This can be explained partially by the different geological strata surrounding the pile. The upper meters of ground are composed of soft clayey materials, which offer less resistance to the dilation of the pile than the gravels existing in the lower meters of the pile.

From the strain data obtained at different depths, the whole elongation of the pile can be calculated. At moment Cb, under the action of a heat injection rate of 120W/m, the pile exhibits a maximum elongation of +1.6 mm. Meanwhile, the maximum pile head vertical movement measured by the LVDT's is +1.23 mm. By comparing these two values (Fig.17), a settlement of the pile toe of 0.37 mm is deduced.
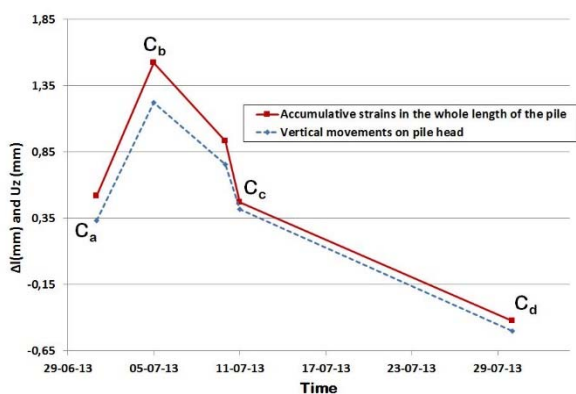
Fig.17. Comparison between the accumulative strains along the pile and the vertical movements measured on pile head

Since part of the pile deformation is constrained by the surrounding soil, a blocked, non-manifested, strain has to be considered:

$$\varepsilon_{th,c} = \varepsilon_{th,f} - \varepsilon_{obs} \qquad (10)$$

Part of the free strain is effectively observed while the remaining part is converted into the internal thermal stress.

Stresses

1. Thermal stresses

The average thermal axial stresses induced in the foundation by the temperature changes (kN) can be calculated from the measured thermal axial strains at the location of each gauge as follows:

$$\sigma_{th} = -E \cdot \varepsilon_{th,c} \qquad (11)$$

where the minus sign represents the convention of negative compression; $\varepsilon_{th,c}$ is the non-produced thermal axial strain (μm/m) and E is the Young's modulus of the pile (31314 MN/m^2).

The calculated thermal (σ_{th}) and total ($\sigma_{th+mec} = \sigma_{mec} + \sigma_{th}$) axial stress profiles are shown in Fig. 18 and 20. In these figures, negative stresses indicate compression while positive values indicate extension.

Comparison of this figure with the evolution of strains allows seeing that the locations of the smallest observed strains in the energy pile (where the pile is surrounded by stiff sands and gravels) correspond to the locations of the maximum thermal axial stresses, possibly due to the resistance to thermal axial expansion by mobilization of shaft shear stresses. In other words, compressive (negative) thermal axial stresses occur during heating of the pile (cooling of the building) when the axial expansion of the foundation is restrained by the ground at the pile/soil interface and at the pile base. Though not clearly visible in Fig. 19, a trend to zero thermal stresses at the head pile exists, due to the lack of restriction to expansion at this point of the pile, since the mechanical load is maintained constant at 1000 kN. (Actually, this trend is much clearer with the OFV results). In Ce, 19 days after end of test C, the stress profile tends to the initial state in the deeper part of the pile, while the first meters show that more time is needed to recover the initial state prior to test C.
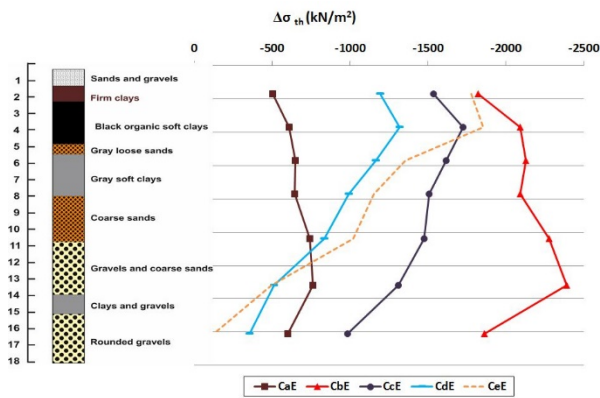
Fig.18. Thermal axial stress due to heating and cooling during test C

2. Total stresses

The thermal axial stress profiles observed during heating and cooling of the pile were superimposed upon the stress profile due to mechanical loading (1000 kN) to define the total thermo-mechanical axial stresses (Fig.19).
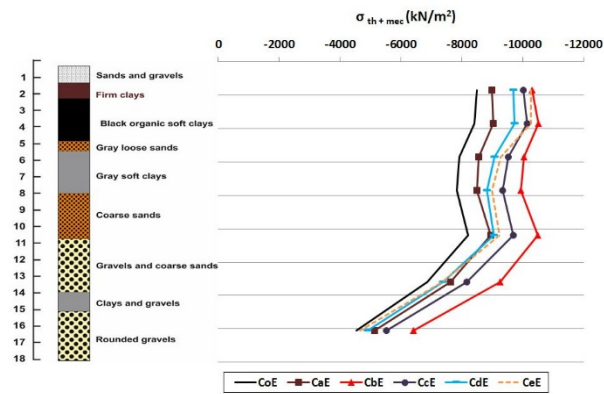
Fig.19. Total axial stress evolution throughout the test C

Two main different zones can be distinguished in the pile: an upper part, between 2m and 10 m of depth, where the surrounding ground consists of soft soils (soft clays, organic clays and loose sands), that shows an almost vertical profile; a lower part of the pile, from about depth -10m, showing a diminishing stress towards the pile toe, as a consequence of the presence of stiff gravels and sands with a higher frictional resistance. Comparing Figs. 19 and 20, it can be seen that the thermal axial stresses are clearly lower than the mechanical axial stresses; nevertheless, they are not at all insignificant (about 2500 kN/m^2 of maximum thermal stress, relatively to 8163 kN/m^2 of maximum mechanical stress).

Loads

The thermal and total stresses profiles can be converted into thermal and total load profiles respectively (Fig. 20 and 21), by simply using the following equation:

$$N = \sigma \cdot S \qquad (12)$$

Where N is the axial load (kN), σ is the average stress in the corresponding section (kN/m^2) and S is the area of the pile section (S = 0.35·0.35 = 0.12 m^2).
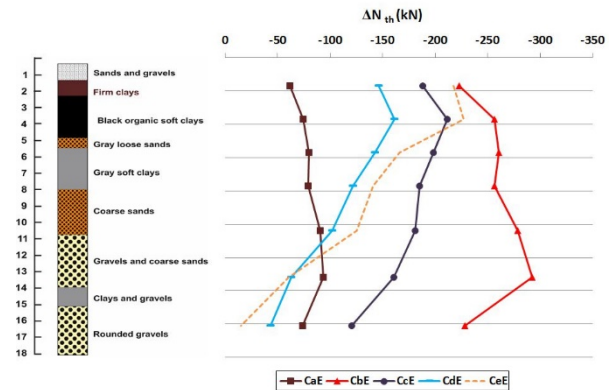
Fig.20. Thermal axial load profiles during test C
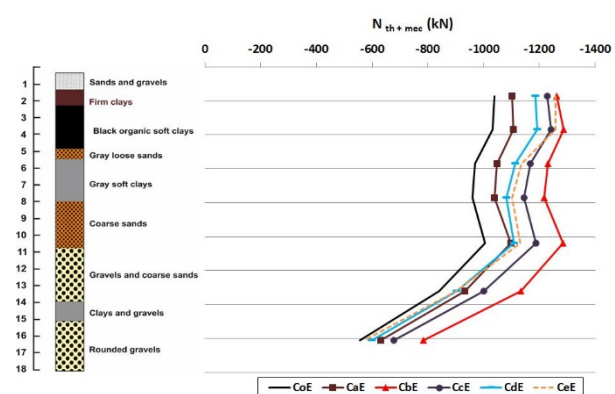
Fig.21. Total axial load profiles during test C

Pile/ soil interface shear stress

It is worthwhile to remark how the thermal and total shear stresses originated along the pile shaft (Fig. 22 and 23) are related to the heat injection in the pile.
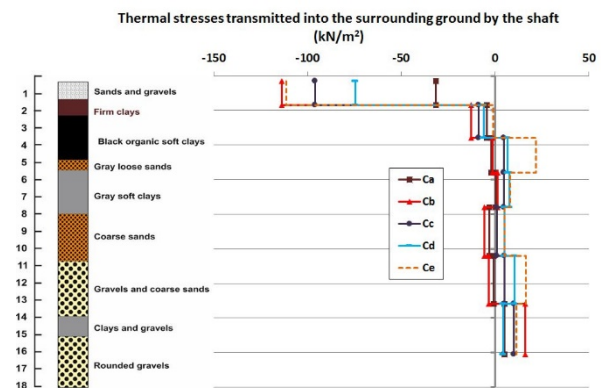
Fig.22. Thermal shear stresses along pile shaft during test C (kN/m^2)
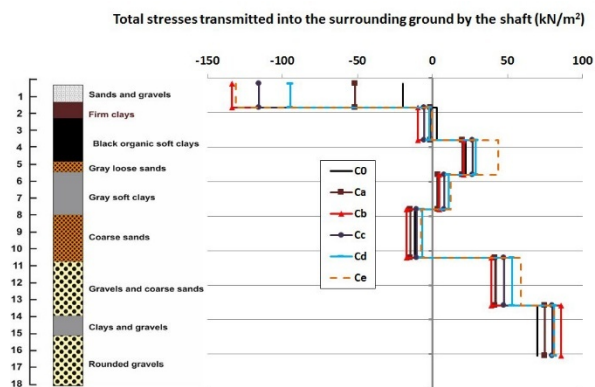
Fig.23. Total shear stresses along pile shaft during test C (kN/m^2)

Heating the pile results in dilatation deformations. As a result of the tendency of the surrounding soil to constrain the pile dilation, the mobilized shaft friction during heating shows an opposite response at the upper part, where the friction is negative (the soil is exerting a downwards force on the pile shaft), and the lower part of the pile, where the friction is positive (the soil is exerting an upwards load on the pile shaft). The resistance to pile stretching is not uniformly distributed along the pile depth, but depends on the ground profile, specifically on the existence of soft or stiff soil levels. Only those layers of stiff or very frictional materials will be able to oppose the pile dilation or contraction. At the depths where the pile is surrounded by soft soils, the opposition to thermal dilation or contraction of the pile will be negligible. In our experiment, it appears that the resistance to pile dilation is concentrated at both ends of the pile, the upper 2 metres, where the soil consists in artificial fills and stiff clays, and at the toe area, where the soil is composed of coarse sands and gravels. This evidences the importance of the stratigraphic column in the thermo-mechanical behaviour of the system.

The described trend towards stretching reverses at Cc and Cd, when the pile cools down with respect to Cb. During this process, the soil tends also to show a stronger opposition to pile contraction at both ends.

In summary, pile/soil interface shear stresses generated due to heat injection into the pile during the test C, are coherent with the theoretical considerations and previous observations, [5], with some specific peculiarities derived from the local geological profile, showing two main zones of stiff lithologies that can constrain the potential pile deformation: the upper 2 metres and the toe zone. During the cooling part of the test C (Cc, Cd moments) the thermal inertia of the soils surrounding the pile are also determinant in the evolution of the profiles.

CONCLUSIONS

This work presents the results from a thermo-mechanical evaluation of a full-scale precast energy pile, under a constant and stable mechanical load of 1000 kN and a wide range of thermal loads, simulating its use within a geothermal installation working on summer mode (cooling the building and heating the foundation).

Data collected from both types of sensors allowed to assess the thermo-mechanical behaviour of the pile in terms of axial strains, stresses and loads, as well as pile/soil interface shear stress values. Thermal and total axial strains measured are consistent with a pile predominantly working at its toe. It is important to notice that the thermal loads applied during the test C, described in this paper, are probably higher than those that would be needed in a real case of geothermal exploration of a normal office or residential building founded on piles like the one used in this study. Nevertheless, the thermal impacts on the mechanical response of the pile would not likely lead to significant structural problems. Anyhow, an analysis of the effects of both the mechanical loads and the thermal loads is considered necessary for a proper design of thermo-active piles.

Further research is still needed to improve the understanding of the thermo-mechanical behaviour of geothermal piles and to formalize design guidelines and safety factors for assuring the ultimate and serviceability limit states of the energy foundations.

ACKNOWLEDGEMENTS

REFERENCES

1 L. Laloui, M. Moreni & L. Vulliet, Can. Geotech. J. 40, 388-402 (2003).
2 L. Laloui, M. Nuth & L. Vulliet, International Journal for Numerical & Analytical Methods in Geomechanics, 30, No 8, 401, (2006).
3 H. Brandl, Geotechnique, 56, No 2, 81, (2006).
4 A. Amis, P. Bourne-Webb, B. Amatya, K. Soga, & C. Davidson, 3rd Ann. and 11th Int. DFI Conf., New York, 10 pp (2008).

5 P. Bourne☐Webb, B. Amatya, K. Soga, A. Amis, C. Davidson & P. Payne, Géotechnique, 59, 237 (2009).

6 L. Laloui & A. di Donna, Civil Engineering, 164, 184, (2011).

7 B.L. Amatya, K. Soga, P. Bourne-Webb, T. Amis & L. Laloui, Géotechnique, 62, 1, (2012).

8 F.A.Loveridge & W. Powrie (2013) Pile heat exchangers: thermal behaviour and interactions. Proceedings of the Institute of Civil Engineers: Geotechnical Engineering, 166, (2), 178-196.

9 K.D. Murphy & J.S. McCartney (2014). "Seasonal Response of Energy Foundations during Building Operation." Geotechnical and Geological Engineering. 1-14.

10 M.E. Suryatriyastuti, H. Mroueh,S. Burlon & J. Habert. Energy Geostructures (2013) Chapter seven

11 Instrucción Española del Hormigón Estructural (EHE-08).

12 Código Técnico de la Edificación – Documento Básico de Seguridad Estructural (DB-SE C, 2006).

13 C. Knellwolf, H. Peron & L. Laloui, Journal of Geotechnical and Geoenvironmental Engineering, 137, No 10, 890 (2011).

14 F. Loveridge, Ground Source Seminar, Homerton College, Cambridge University, (2011).

15 GSHPA Association. Thermal pile design, installation and material standards. Issue 1.0, 1st October 2012.

16 Eskilson, P., (1987). Thermal Analyses of Heat Extraction Boreholes. Ph.D. Thesis. Department of Mathematical Physics, Lund Institute of Technology, Box~118, S-221~00 Lund, Sweden.

17 Gehlin S. 2002. Thermal Response Teast, Meathod Development and Evaluation. Doctoral Thesis 2002:39. Luleå University of Technology. Sweden.

18 D.J. Lennon, E. Watt & T.P. Suckling, Proceedings of the Fifth International Conference on Deep Foundations on Bored and Auger Piles (Eds: Taylor & Fran-cis Group, ed), 15 May 2009 Frankfurt., London.

19 C.J. Wood, H. Liu & S.B. Riffat, International Journal of Low-Carbon Technologies, 5, 137, 2010.

20 H. Park, S.R. Lee, S. Yoon & J.C. Choi, Applied Energy, 103, 12, (2013).

21 J.S. McCartney & K. Murphy, DFI Journal, 6 No 2, 26, 2012.

22 H. Peron, C. Knellwolf & L. Laloui, L, GeoFrontiers, ASCE, 470, 2011.